

LETTERS

Hydrogen Bond Dynamics in Water and Ultrafast Infrared Spectroscopy

Rossend Rey,[†] Klaus B. Møller,^{*,‡,§} and James T. Hynes^{‡,||}

Departament de Física i Enginyeria Nuclear, Universitat Politècnica de Catalunya, Campus Nord B4-B5, Barcelona 08034, Spain, Département de Chimie, Ecole Normale Supérieure, 24 rue Lhomond, 75231 Paris Cedex 5, France, Department of Chemistry, Technical University of Denmark, DK-2800 Kgs. Lyngby, Denmark, and Department of Chemistry and Biochemistry, University of Colorado at Boulder, Boulder, Colorado 80309

Received: July 1, 2002; In Final Form: October 29, 2002

Molecular dynamics simulations are used to examine two key aspects of recent ultrafast infrared experiments on liquid water dynamics. It is found that the relation between the OH stretch frequency and the length of the hydrogen bond in which the OH is involved, currently assumed to be one-to-one, is instead characterized by considerable dispersion and that the time scale currently interpreted in terms of a stochastic modulation by the surrounding solvent of a highly frictionally damped hydrogen bond system is shown to be governed by hydrogen bond-breaking and -making dynamics, whereas the motion of an intact hydrogen-bonded complex is underdamped in character.

In view of the obvious importance of liquid water in chemistry and physics, its microscopic dynamics have long been of major interest. Recently, modern ultrafast spectroscopic methods have opened a new experimental window on these dynamics, and there has been intensive activity on unravelling water dynamics via examination of the experimentally convenient aqueous system of HOD diluted in D₂O using either ultrafast infrared (IR),^{1–6} IR–Raman,⁷ or photon echo^{8,9} spectroscopy.

One focus of these experiments has been the excited OH vibration population lifetime, which is currently interpreted as being dominated by either vibrational predissociation,¹ i.e., the breaking of the hydrogen bond (H bond) in which the excited OH stretch is involved,¹⁰ or by vibrational relaxation of the excited OH vibration without such IR-induced bond breaking.^{7,11} A second focus, of interest here, has concerned the spectral

diffusion within the OH stretching band,^{2–6} initially discussed in terms of the dynamics of the H bond DOH...OD₂ (hereafter OO H bond) in terms of the time evolution of this bond initially prepared in a nonequilibrium stretched/compressed condition^{3–6} and subsequently discussed more formally in terms of stochastic models which assume strongly overdamped motion of the oscillator.

A striking aspect of the current interpretations of such experiments concerning the presumed intact OO H-bond dynamics is that the OO motion is inferred to be highly overdamped. For example, an H bond initially stretched beyond its equilibrium length will, on average, monotonically relax to equilibrium, without oscillation (see, e.g., Figure 3 of ref 3 and the discussion therein). Further, subsequent discussions all invoke a highly overdamped character of the H-bond motion.^{3–6} In our view, this is surprising because the H bond is estimated in H₂O to have a reasonably high frequency ~200 cm⁻¹,¹² and an extremely high friction would be required to produce highly overdamped motion. To examine this issue, we have performed molecular dynamics (MD) simulations of an

* To whom correspondence should be addressed.

[†] Universitat Politècnica de Catalunya.

[‡] Ecole Normale Supérieure.

[§] Technical University of Denmark.

^{||} University of Colorado at Boulder.

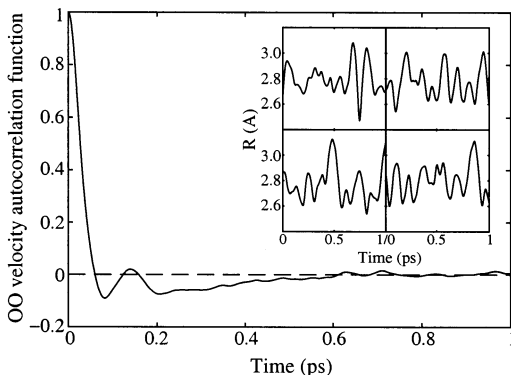


Figure 1. Normalized velocity autocorrelation function for the OO distance R between HOD and a D_2O molecule initially its nearest neighbor. Note the oscillatory behavior, with a frequency $\sim 200\text{ cm}^{-1}$. Inset: Four trajectories $R(t)$, chosen arbitrarily, with the condition that the two molecules remain nearest neighbors for 1 ps. The clearly underdamped motion has an amplitude of $\sim 0.4\text{ \AA}$.

equilibrium system (298 K) of an HOD molecule in liquid D_2O (simulation details are given below), focusing on the OO H-bond dynamics. Figure 1 shows, for both the calculated velocity autocorrelation function and individual trajectories, that the OO vibration is decidedly not overdamped.¹³

In view of this discrepancy, it is natural to scrutinize aspects of the discussion of the experiments which may not be valid or which require clarification. In particular, we examine two key features. The first is the assumption employed in the discussion of the experiments that there is a one-to-one correspondence between the frequency ω_{OH} of the OH vibration and the OO distance R in a HOD- D_2O pair. Although this type of relation, in which ω_{OH} decreases with decreasing R , as the H-bond strength is increased, is well established *on the average* for a wide variety of static systems,^{14,15} it may not be sufficiently sharp to use in the context of the dynamic spectroscopic experiments.⁸ The second aspect concerns the interpretation of the dynamics being probed during the experimental time window ($\sim 1\text{--}2\text{ ps}$). Although this has been discussed in terms of diffusive or high friction “Brownian oscillator” stochastic models,^{3–6} it seems fair to say that a clear identification of the dynamics and measured time scales has not yet been achieved. However, it has been noted^{4,9} that the experimental time scale ($\sim 500\text{--}700\text{ fs}$) is the same order of magnitude as the estimated lifetime of an H bond in liquid H_2O .¹⁶ We will conclude via the results presented within that the one-to-one frequency-H-bond length assumption is not valid and that the observed experimental time scale should be interpreted in terms of H-bond-breaking and -making dynamics.

MD simulation of 3 ns duration, preceded by an initial 15 ps equilibration run, has been applied to a system of one HOD molecule in 107 D_2O molecules. We adopt the SPC/E model for intermolecular interactions and molecular geometry,¹⁷ without internal motions (imposed via the “shake” algorithm). The simulation box dimensions yield a density 1.104 g/cm^3 . A molecular spherical cutoff at half the box length was used for all forces, and the Ewald summation procedure was applied for electrostatic forces. The integration algorithm is of the leapfrog type¹⁸ (1 fs time step) with thermal bath coupling (mean temperature 298 K, coupling constant 0.5 ps).

The calculations presented below involve the OH stretch frequency, which is probed in the experiments. Given the local nature of the HOD molecule vibrations,^{11,19} the OH coordinate has been approximated as an independent vibrational mode. The Reimers–Watts internal local mode potential,¹⁹ used here for

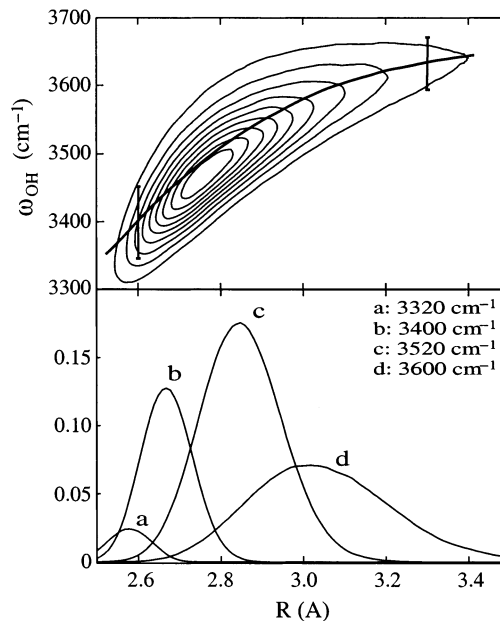


Figure 2. Top: Density-of-states histogram for the OO distance R between HOD and its nearest neighbor and the OH frequency ω_{OH} (contour levels are 10%, 20%, ..., 90% of maximum value). Also shown, the average ω_{OH} for a fixed R ($\pm 0.01\text{ \AA}$) and the fwhms in ω_{OH} for $R = 2.6\text{ \AA}$ (200 cm^{-1}) and $R = 3.3\text{ \AA}$ (150 cm^{-1}), both being larger than typical laser bandwidths $\sim 70\text{ cm}^{-1}$.^{3–5} Bottom: Probability distribution of R for fixed values of ω_{OH} ($\pm 5\text{ cm}^{-1}$). Our results use instantaneous shifts, without motional narrowing.²³

the frequency shifts computation, yields a gas-phase variational OH frequency 3725 cm^{-1} if the other modes are frozen, acceptably close to the experimental value 3707 cm^{-1} .²⁰ The vibrational problem is exactly solved in the Born–Oppenheimer approximation of a fast vibration and a slow “bath”, which is reasonable given the high OH frequency.^{11,21,22} At each simulation time step, the OH vibrational coordinate q has been assigned expanded and contracted values, with the remaining degrees of freedom kept at their instantaneous values. For each value of q , the total energy is computed, resulting in a q -dependent perturbation which, together with the intramolecular gas phase potential, constitutes the exact instantaneous vibration potential. The resulting vibrational Schrödinger equation is solved numerically.²¹

We begin the discussion of the HOD in D_2O OH frequency results with Figure 2, which displays the density-of-states histogram of the OO distance and the instantaneous frequency ω_{OH} , as well as the corresponding probability distribution in R for different ω_{OH} . The distribution of instantaneous frequencies itself (not shown) has the center frequency 3516 cm^{-1} and the full width at half-maximum (fwhm) 240 cm^{-1} (the experimental spectrum gives 3420 and 260 cm^{-1} , respectively²⁴). Figure 2 shows a general trend of higher frequency (smaller red shift with respect to gas-phase value) with increasing R , consistent with weaker H bonding at larger R . However, for a given ω_{OH} , the distribution in R is quite broad. It is most disperse at high frequencies, for which there are more loosely H-bound configurations: at $\omega_{OH} = 3400\text{ cm}^{-1}$, the fwhm in R is 0.15 \AA ; at $\omega_{OH} = 3600\text{ cm}^{-1}$, it is 0.4 \AA . Hence, in contrast to standard assumption, the ω_{OH} – R relation is far from being sharply defined; indeed, on the blue side, the fwhm in R is comparable to the oscillatory OO motion amplitude (cf. Figure 1).

The solid hydrate experimental data for the ω_{OH} – R_{eq} relation are in fact quite scattered,^{14,15} and H-bond bending has been mentioned as a possible source.¹⁵ We explore this possibility

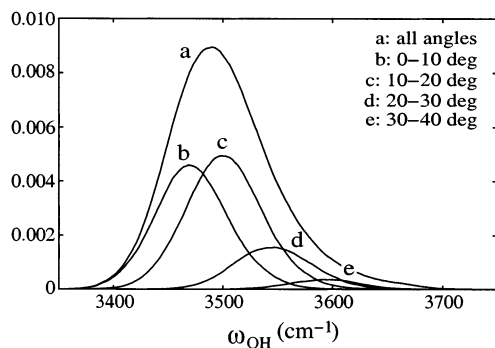


Figure 3. Probability distribution of ω_{OH} for HOD–D₂O pairs with the OO distance $R = 2.8 \pm 0.01$ Å and its separation into different bending angle α intervals.

via Figure 3, which shows the frequency distribution for a fixed nearest-neighbor OO distance, separated into different bending angle α intervals. Overall, there is a clear dependence of α on the OH frequency, with the general trend that a larger α leads to a higher ω_{OH} (smaller red shift), as expected for progressively weaker H bonds. However, the key lesson in Figure 3 is that the bending angle is very clearly a source of significant dispersion in the $\omega_{\text{OH}}-R$ relationship. There can however be further dispersion sources: simulation results (not shown) indicate that indeed the HOD–nearest-D₂O-neighbor interaction is most important but that the orientation of the deuterium atoms on that D₂O can play a role, an issue to be investigated in the future.

To both illustrate the impact of the $\omega_{\text{OH}}-R$ dispersion and to examine the possible role of OO H-bond breaking dynamics for ultrafast IR experiments, we calculate a quantity related to the portion⁵ of the experimental IR signal associated with the ground OH vibrational state hole dynamics, i.e., the time dependence of the average OH frequency $\bar{\omega}_{\text{OH}}(t)$ for the distribution of OH frequencies initially created from an equilibrium distribution by excision of a band of ω_{OH} values corresponding to laser promotion to the vibrationally excited OH state. This average frequency function is complimentary to the one extracted from experiment in ref 5, in which the effect of the excited state is removed, and is closely related to the one reported in refs 3 and 4, where both ground and excited-state contributions are present. The laser pulse time duration is ignored, and the laser promotion is mimicked by assigning to each configuration in the equilibrium distribution at time zero the probability $1 - f(\omega_{\text{OH}})$, where $f(\omega)$ is the laser pulse frequency profile, taken to be a Gaussian with fwhm 70 cm^{-1} . We simulate excitations to the blue and to the red by offsetting the carrier frequency in $f(\omega)$ by $\pm 100 \text{ cm}^{-1}$ with respect to the calculated ω_{OH} spectrum's center.

The results are displayed in Figure 4, in which we have subtracted from $\bar{\omega}_{\text{OH}}(t)$ the average OH frequency ω_{ref} without laser promotion ($f=0$). For the blue (red) excitation, the average frequency $\bar{\omega}_{\text{OH}}$ of the initial ensemble is less (greater) than that of the equilibrium ensemble, because more weakly (strongly) H-bonded species have been excised. As this hole is filled in with more weakly (strongly) H-bonded species, the average frequency increases (decreases). Both excitation results are mildly bimodal in time, a feature also seen in different but related water simulations,²⁵ with a slightly oscillatory feature present for the latter. Analysis of these curves yields for the short time scale 66 (blue) and 31 fs (red) and for the long time scale 863 (blue) and 496 fs (red). In the IR experiments, only a single longer time scale is extracted, estimated variously as $700^{3,4}$ or 500 fs^5 , this difference being related to the different

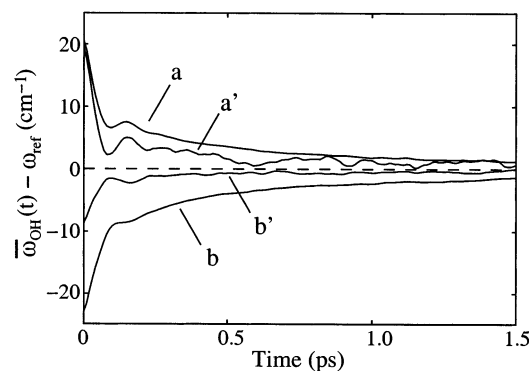


Figure 4. Time dependence of the average OH frequency $\bar{\omega}_{\text{OH}}(t)$ for the distribution of ω_{OH} initially created from an equilibrium distribution by excision of a band of ω_{OH} values corresponding to laser promotion to the vibrationally excited OH state (see text). Curves a and b: excitation to the red and blue, respectively; curves a' and b': the corresponding curves for subensembles containing only H-bonded HOD–D₂O pairs. The quantity ω_{ref} refers to the average OH frequency for the respective (sub-)ensemble without laser promotion.

experiments involved and the differing details of extraction of this time.^{3–5} The slight oscillation for the red excitation result could be quite difficult to detect because of current experimental time resolution capabilities and other contributions to the signal.^{3–5} Note that, although not possible to resolve in IR experiments, a short-time component has been recently observed in photon echo experiments.^{8,9} (Such a short time component in a fluctuating frequency autocorrelation function, which we have also observed in a separate calculation, not shown here, indicates a significant homogeneous broadening.^{8,9})

The fundamental interpretation of the above curves is revealed more clearly when we examine the corresponding dynamics subject to the restriction that only initially OO H-bonded molecular pairs which remain intact up to $t = 2 \text{ ps}$ are involved (we use a geometrical definition of an OO H bond²⁶ in a HOD–D₂O pair: OO distance less than 3.6 Å, distance from H to O in D₂O less than 2.4 Å, and bending angle α less than 30 degrees). For both excitations, the OH frequency averages in this sub-ensemble (cf. Figure 4) display two important features: (i) oscillatory behavior is more clearly pronounced for these intact species than for the full averages and (ii) the long-time component of the full averages has largely disappeared. These results indicate (i) that in the intact OO H-bonded species sub-ensemble, the underdamped motion is visible, despite the $\omega_{\text{OH}}-R$ relation dispersion, a conclusion confirmed by calculation (not shown) of the H-bond length R dynamics in the sub-ensemble, and (ii) that the longer time dynamics in the full averages is determined by H-bond-breaking and -making dynamics; it is not, for example, determined by the overdamped motion of intact H-bonded species. Indeed, the characteristic time ($\sim 0.5-1 \text{ ps}$) of the longer time component is in the range of previous estimates of the thermal lifetime of H bonds in liquid H₂O.¹⁶ (Although not presented here, our analysis of the calculated fluctuating frequency equilibrium time correlation function^{8,9,27} shows this same longer time scale behavior associated with H-bond-breaking and -making.)

Finally, we have examined these issues by following in time the OO distance $R(t)$ for ensembles of initially H-bonded HOD–D₂O pairs with a given $R(0)$. Figure 5, for the case $R(0) = 2.7$ Å, shows the ensemble averaged OO distance, as well as the averages for the two sub-ensembles composed of trajectories for which at any time t , $R(t)$ is respectively less than or greater than the full ensemble average value. This decomposition clearly shows bound oscillatory behavior for the former and divergent,

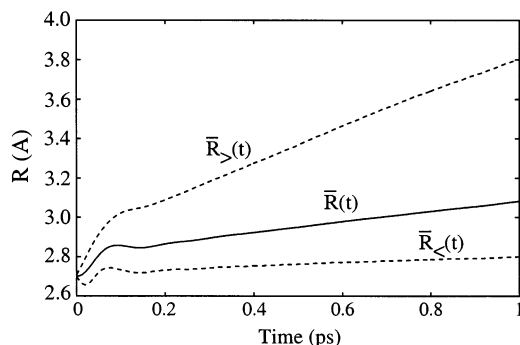


Figure 5. Average of the time-dependent OO distance $R(t)$ for an ensemble of HOD–D₂O pairs with fixed initial OO distance $R(0) = 2.7 \pm 0.01$ Å (solid curve); averages for the two sub-ensembles composed of trajectories for which at any time t , $R(t)$ is respectively less than or greater than the full ensemble average value (dotted curves).

dissociating behavior for the latter, completely consistent with the picture from the hole dynamics.²⁸

To summarize, MD simulations for the HOD dilute in liquid D₂O system have indicated very significant departures from the one-to-one correspondence between the OH vibrational frequency ω_{OH} and the OO hydrogen bond length R assumed in current interpretations of ultrafast infrared spectroscopic experiments. This dispersion is dominated by the dispersion of the H-bond OHO angle, with further contributions arising from (especially) differing OD bond orientations in the D₂O partner and from the surrounding D₂O molecules. Thus, spectroscopic selection of a given ω_{OH} value should be interpreted as providing a significant range of H-bond distances, rather than a unique one. Although this feature obscures to some degree the underdamped character of the OO H-bond motion in an intact species, it does not obliterate it. More importantly, we have argued that the longer time dynamics are associated with the breaking and making of H bonds. Thus, for example, a spectroscopic interpretation in terms of an intact OO H-bonded species would not be appropriate. These features need to be taken into account in experimental interpretations, as well as in a more complete theoretical treatment, including both ground and excited OH states, currently underway.

Note Added in Proof

Related conclusions have been reached by J. Skinner.²⁹

Acknowledgment. This work was supported by EC TMR network HPRN-CT-2000-19, MCYT project BFM2001-2077, the CNRS, and NSF Grant CHE-0108314.

References and Notes

- (1) Woutersen, S.; Emmerichs, U.; Nienhuys, H.-K.; Bakker, H. J. *Phys. Rev. Lett.* **1998**, *81*, 1106. Nienhuys, H.-K.; Woutersen, S.; van Santen, R. A.; Bakker, H. J. *J. Chem. Phys.* **1999**, *111*, 1494.
- (2) Laenen, R.; Rauscher, C.; Laubereau, A. *Phys. Rev. Lett.* **1998**, *80*, 2622. Laenen, R.; Rauscher, C.; Laubereau, A. *J. Phys. Chem. B* **1998**, *102*, 9304.
- (3) Gale, G. M.; Gallot, G.; Hache, F.; Lascoux, N.; Bratos, S.; Leicknam, J.-C. *Phys. Rev. Lett.* **1999**, *82*, 1068.
- (4) Bratos, S.; Gale, G. M.; Gallot, G.; Hache, F.; Lascoux, N.; Leicknam, J.-C. *Phys. Rev. E* **2000**, *61*, 5211.
- (5) Woutersen, S.; Bakker, H. J. *Phys. Rev. Lett.* **1999**, *83*, 2077.
- (6) Bakker, H. J.; Woutersen, S.; Nienhuys, H.-K. *Chem. Phys.* **2000**, *258*, 233. Gallot, G.; Lascoux, N.; Gale, G. M.; Leicknam, J.-C.; Bratos, S.; Pommeret, S. *Chem. Phys. Lett.* **2001**, *341*, 535. Bakker, H. J.; Nienhuys, H.-K.; Gallot, G.; Lascoux, N.; Gale, G. M.; Leicknam, J.-C.; Bratos, S. *J. Chem. Phys.* **2002**, *116*, 2592.
- (7) Deak, J. C.; Rhea, S. T.; Iwaki, L. K.; Dlott, D. D. *J. Phys. Chem. A* **2000**, *104*, 4866.
- (8) Stenger, J.; Madsen, D.; Hamm, P.; Nibbering, E. T. J.; Elsaesser, T. *Phys. Rev. Lett.* **2001**, *87*, 027401.
- (9) Stenger, J.; Madsen, D.; Hamm, P.; Nibbering, E. T. J.; Elsaesser, T. *J. Phys. Chem. A* **2002**, *106*, 2341.
- (10) Staib, A.; Hynes, J. T. *Chem. Phys. Lett.* **1993**, *204*, 197.
- (11) Rey, R.; Hynes, J. T. *J. Chem. Phys.* **1996**, *104*, 2356.
- (12) Souaille, M.; Smith, J. C. *Mol. Phys.* **1996**, *87*, 1333 and references therein.
- (13) In this connection, it is of interest to note that underdamped H-bond motion is assumed in the theoretical work of one of us on proton-transfer reactions in solution (see, e.g., Kiefer, P. M.; Hynes, J. T. *J. Phys. Chem. A* **2002**, *106*, 1850) and that oscillations have been experimentally observed for an intramolecular H bond in Stenger, J.; Madsen, D.; Dreyer, J.; Nibbering, E. T. J.; Hamm, P.; Elsaesser, T. *J. Phys. Chem. A* **2001**, *105*, 2929.
- (14) Mikenda, W. *J. Mol. Struct.* **1986**, *147*, 1. Mikenda, W.; Steinböck, S. *J. Mol. Struct.* **1996**, *384*, 159.
- (15) Libowitzky, E. *Monatsh. Chem.* **1999**, *130*, 1047.
- (16) Luzar, A. *J. Chem. Phys.* **2000**, *113*, 10663.
- (17) Berendsen, H.; Grigera, J.; Straatsma, T. *J. Phys. Chem.* **1987**, *91*, 6269.
- (18) Berendsen, H.; Postma, J.; van Gunsteren, W.; DiNola, A.; Haak, J. *J. Chem. Phys.* **1984**, *81*, 3684.
- (19) Reimers, J.; Watts, R. *Mol. Phys.* **1984**, *52*, 357.
- (20) Benedict, W. S.; Gailar, N.; Plyler, E. *J. Chem. Phys.* **1956**, *24*, 1139.
- (21) Rey, R.; Hynes, J. T. *J. Chem. Phys.* **1998**, *108*, 142.
- (22) Ojamae, L.; Hermansson, K.; Probst, M. *Chem. Phys. Lett.* **1992**, *191*, 500.
- (23) Ojamae, L.; Tegenfeldt, J.; Lindgren, J.; Hermansson, K. *Chem. Phys. Lett.* **1992**, *195*, 97.
- (24) Falk, M.; Ford, T. *Can. J. Chem.* **1966**, *44*, 1699.
- (25) Diraison, M.; Guissani, Y.; Leicknam, J.-C.; Bratos, S. *Chem. Phys. Lett.* **1996**, *258*, 348.
- (26) Luzar, A.; Chandler, D. *J. Chem. Phys.* **1993**, *98*, 8160.
- (27) Georgievskii, Y.; Marcus, R. A. *J. Phys. Chem. A* **2001**, *105*, 2281.
- (28) We have also found by computation that the autocorrelation function for an initial equilibrium ensemble of $\Delta R(t) = R(t) - R_{eq}$, where R_{eq} is the equilibrium separation for an intact H-bonded species, is divergent on longer time scales for the same reason.
- (29) Skinner, J. I. (Wisconsin), private communication.